



Simulation of Complete Dual Compressor Turbojet Engine with Combustion

R. Ševčík*

*PBS Velka Bites, a.s., Vlkovska 279, Velka Bites, Czech Republic
Department of Aircraft Technology, University of Defence, Brno, Czech Republic*

The manuscript was received on 27 September 2023 and was accepted after revision for publication as a case study on 1 March 2025.

Abstract:

This article presents a comprehensive study on the simulation of a complete dual compressor turbojet engine with combustion. The engine model consists of a single-stage axial compressor, a single-stage radial compressor, a combustion chamber, and a single-stage axial turbine. The simulation of the complete engine allows for the consolidation of boundary conditions and input parameters, resulting in more accurate information transfer between different segments. The study contributes to advancements in engine design, performance optimization, and the broader understanding of similar propulsion systems. The methodology, boundary conditions, challenges faced, and results obtained from the simulations are discussed in detail. The successful creation of the model demonstrates its potential for optimizing engine components and studying their behavior under various flight conditions.

Keywords:

dual compressor turbojet engine, ANSYS fluent, simulation, combustion, complete engine model, aerospace engineering

1 Introduction

This article presents a comprehensive study based on commercial development of a dual compressor turbojet engine, highlighting its configuration, performance characteristics, and the benefits of simulating the complete engine. The information discussed in this article is limited due to the ongoing nature of the commercial development process.

Creating a numerical simulation of a jet engine or its components is not always straightforward. Even with well-tested and functioning equipment, where the underlying physics is reliable and the engine or its parts operate as expected, finding the

* Corresponding author: Department of Aircraft Technology, University of Defence, Kounicova 156/65, CZ-662 10 Brno, Czech Republic. Phone: +420 603 16 16 76, E-mail: radek.sevcik@unob.cz

correct computational setup can be challenging. It often involves testing various mesh configurations, and the results of the simulation may not always align with actual measurements. This article describes the development of a model not just for a single part of a jet engine, as is commonly done, but for the entire engine, including the simulation of fuel combustion. Building such a comprehensive model and achieving numerical convergence was a challenging task. Successful completion of this task marks a significant achievement, demonstrating the feasibility of such detailed simulations.

The modeled engine consists of a single-stage axial compressor, a single-stage radial compressor, a combustion chamber, and a single-stage axial turbine. With a thrust range of 2 to 3 kN, this type of engine is commonly utilized in applications such as drones, target drones, and small guided missiles. The engine under development requires parameter optimization and specific features, including the ability to operate efficiently at high altitudes. Traditionally, individual components of such engines are analyzed independently, focusing solely either on the compressor or the turbine, for example.

However, these isolated component calculations often suffer from inaccuracies as a result of manually estimating and inputting various boundary conditions and input parameters specific to each segment. Simulation of the complete engine allows for the consolidation of these conditions, enabling the transfer of more accurately computed information between different segments. By simulating the entire engine, a better understanding of the underlying physical processes within the engine can be obtained, leading to improved parameter optimization. Moreover, the comprehensive model facilitates a wide range of sensitivity analyses, enabling an exploration of the effects of varying parameters on the engine's behavior under different operating conditions and flight regimes.

The simulation of the entire engine has not been utilized for parameter optimization to date. While development of the engine continues at PBS, the comprehensive model described in this article has not been deployed, likely due to the specialized expertise required and the complexity of the model, which exceeds current operational requirements. Nevertheless, the author has obtained permission from the company's management to publish this article, contributing to the broader academic and engineering discussions on this topic.

The results obtained from these simulations can be applied to design modifications for the specific engine under development. Furthermore, after generalization, the findings can be extended to other similar engines and devices, such as auxiliary power units (APUs), amplifying their impact in the field of aerospace engineering.

2 Methodology and Boundary Conditions

As part of the development process for a new jet engine, our results have contributed to the computational analysis of its individual components, specifically focusing on verification calculations and optimizing the flow path geometries (Fig. 1).

We began by modeling each component, including the axial compressor, radial compressor, nozzle turbine, and finally, the combustion chamber, along with simulating the combustion process [1-3]. However, simulating the combustion chamber posed a challenge in accurately specifying the inlet parameters. Given the well-calculated individual components, we conceived the idea of integrating them into a cohesive

model, eliminating the issue of precisely setting the boundary conditions at the inlet and outlet of each segment.

We proceeded step by step, initially combining the inlet section, axial compressor, connecting duct, radial compressor, and diffuser into a single model. This first model terminated at the outlet to the combustion chamber, and it underwent meticulous refinement until achieving excellent convergence.

Since we had previously modeled both the combustion chamber and the turbine with the nozzle separately, we integrated these segments into a unified model. Initially, we fine-tuned the model for cold flow without considering combustion, and subsequently, we successfully refined the model to include combustion simulation. The non-premixed combustion model was used for calculating the combustion process, requiring the computation of a probability density function table.

Having successfully computed the first and second halves of the jet engine independently, it was time to merge all segments into a comprehensive whole. This integration was accomplished, and the calculation of cold flow without combustion on the complete engine model exhibited excellent convergence.

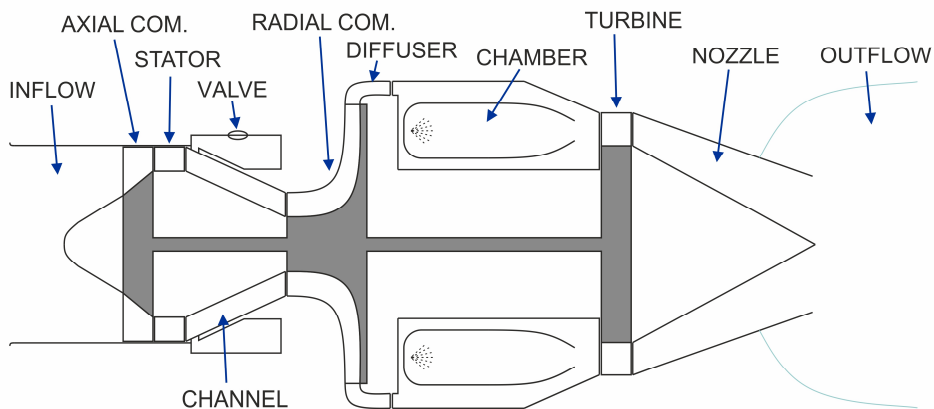


Fig. 1 The schematic diagram illustrates the individual parts of the engine

Unfortunately, when the combustion simulation was activated, the calculation diverged, and stabilizing the computation became a challenge. The non-premixed combustion method did not work for the complete engine model in the Steady, Steady pseudo-transient, or transient modes. However, this method proved successful when applied solely to the combustion chamber or to the combustion chamber with the turbine.

Following consultations with colleagues and technical support from ANSYS, we utilized the Species Transport method with the Eddy Dissipation turbulence-chemistry interaction model. This approach enabled the stabilization of the computation and achieved convergence. Once the computation stabilized, it was necessary to switch to the Finite-Rate option, which provided better accuracy. However, even with this configuration, the task was highly sensitive, and the relaxation factors had to be set very low, typically around 0.01 to 0.03, to prevent divergence.

Throughout the computation, various monitored parameters, including continuity, pressure, flow rates across segments, temperature, velocity, segment balances, overall flow rate, compression rate of the axial and radial compressors, and expansion ratio in

the turbine, approached their expected values after approximately 10 000 iterations. During the design phase of the jet engine, each component was engineered to achieve specific operational values for pressure, efficiency, and other physical parameters. The values of these physical quantities in the numerical simulation of the entire engine approached the expected design values after approximately 10 000 iterations. This convergence towards the design specifications demonstrates the accuracy and effectiveness of the simulation model in replicating the anticipated performance of the engine.

Each segment of the model features specific surfaces where physical quantities such as temperature, pressure, and flow velocity are evaluated. Typically, these measurement surfaces are located at key points such as the inlet and outlet, before and after the compressor or turbine blades, or at positions where sensors are commonly placed during testing. The model comprises a total of 11 segments, with approximately 3-4 evaluation surfaces per segment, cumulatively amounting to 37 significant surfaces across the entire engine model, see Tab. 1. The calculation was considered complete when the values of all critical variables stabilized.

Critical variables in this context are considered to be quantities that are crucial for determining key performance metrics, such as efficiency. These include total and static pressure, pre-turbine temperature (to prevent turbine damage), and other quantities whose values directly influence the overall operation of the engine. The stabilization of these critical variables is essential for ensuring the engine’s performance aligns with design expectations and safety standards.

Tab 1 Partial list of significant surfaces.

N.	Surface Name	Segment Name	Description
1	vstup	inflow	segment inlet
2	z1	inflow	in front of cone
3	mp01	inflow	segment outlet
4	mp02	axial	segment inlet
5	z2	axial	in front of blade
...			
31	z15	turbine	behind blade
32	mp15	turbine	segment outlet
33	mp16	nozzle	segment inlet
34	z16	nozzle	inside nozzle
35	z17	nozzle	inside nozzle
36	z18	nozzle	inside nozzle
37	vystup	nozzle	segment outlet

The entire model used a polyhedral mesh type with a boundary layer. The total number of cells in the model was about 13.9 million, see Tab 2. The settings for the boundary layer, cell sizes, and growth rate were optimized based on previous models. The turbulence model was selected based on prior calculations performed on other

engines, allowing for comparison between computation and measurements on a real engine.

During the sensitivity analysis conducted on the compressors of other engines, several turbulence models were tested [4]. The k-Omega SST model demonstrated the best agreement with the measurements and was subsequently used for the complete engine model as well. This model was configured with options such as Viscous Heating, Curvature Correction, Compressibility Effects, and a Production Limiter enabled. It is important to note that while this model may be optimal for a compressor with a specific geometry, it may not necessarily be the best choice for a turbine. Optimizing the appropriate turbulence model exceeds the scope of this work and could be the subject of further study.

This approach led to the selection of the most suitable turbulence model and its settings, resulting in the closest agreement between the computed and measured performance of the jet engine. Boundary conditions were set at the inlet and outlet of the engine, which remained the same for zero altitude and zero velocity conditions. This configuration corresponded to the test facility scenario. No additional boundary conditions needed to be specified. If we wished to analyze the engine's behavior under different flight conditions, we would simply adjust the inlet and outlet conditions accordingly.

The ANSYS Fluent 2022 R1 software was used for the computations. The calculations were performed on multiple computers, depending on the available computational capacity. The RAM memory consumption during the computation was approximately 100 GB. On a typical high-performance computer, the calculation progressed at a rate of approximately 40 iterations per hour. Several dozen different computation configurations were tested before finding the setup that resulted in convergence.

The following computational configurations were tested during the development of the engine model:

- steady state simulation with default Under-Relaxation Factors,
- pseudo-transient simulation with automatic stepping and manual time step adjustments.

The final configuration utilized was a steady state model with a Flow Courant Number set to 1. The Under-Relaxation factors were progressively reduced until a compromise was achieved where the computation ran relatively quickly but did not diverge, maintaining stability at a value of 0.02 for all variables. Due to computational constraints, it was not feasible to experiment with individual relaxation factors for each variable separately.

The graphs depict the convergence profiles of flow rate, temperature, overall flow rate, and compression in the first half of the computation (first 6 000 iterations) at significant planes. To maintain confidentiality of the industrial design, the values on the Y-axis are provided in relative units [%].

Figs 2 and 3 illustrate the initial convergence trends of total pressure and temperature, which are commonly used as primary indicators of the convergence in numerical simulations. A well-designed model should prevent pressure values from exploding to nonsensical levels, a common early sign of divergence in simulations. For Figs 2 and 3, the red line represents values at the plane behind the blades of the axial compressor. The green line in Fig. 2 is located in the middle of the connecting duct between the axial and radial compressors, while in Fig. 3, it appears behind the blades of the radial compressor. The blue line shows values behind the blades of the radial diffuser, and

the yellow line indicates values behind the turbine blades. These surfaces were selected to highlight critical areas within different parts of the engine where dynamic changes occur and where numerical instabilities may arise, increasing the risk of divergence. Thus, monitoring these areas is crucial. In Fig. 2, the convergence of flow values in the earlier parts of the engine can be seen aligning gradually, whereas the flow in the turbine significantly deviates. However, as the calculation progresses beyond 10 000 iterations, the flow value at the turbine begins to align with those in the front sections of the engine. Ideally, all these values should be identical; however, due to the inherent errors in numerical simulation, some deviation always exists. As the computation converges, the error decreases, and accuracy improves.

Tab 2 List of segments and their sizes

Nr.	Segment Name	Polyhedral cells per segment	Periodicity number (x)	Periodicity angle [°]
1	INFLOW	283 388	10	36.000
2	AXIAL COM.	421 801	10	36.000
3	STATOR	394 084	14	25.714
4	CHANNEL	62 421	13	27.692
5	VALVE	108 789	13	27.692
6	RADIAL COM.	512 113	13	27.692
7	DIFUSSER	826 864	21	17.143
8	CHAMBER	10 415 632	5	72.000
9	TURBINE	590 177	13.5	26.667
10	NOZZLE	65 026	13.5	26.667
11	OUTFLOW	243 097	13.5	26.667
	Total	13 923 392		

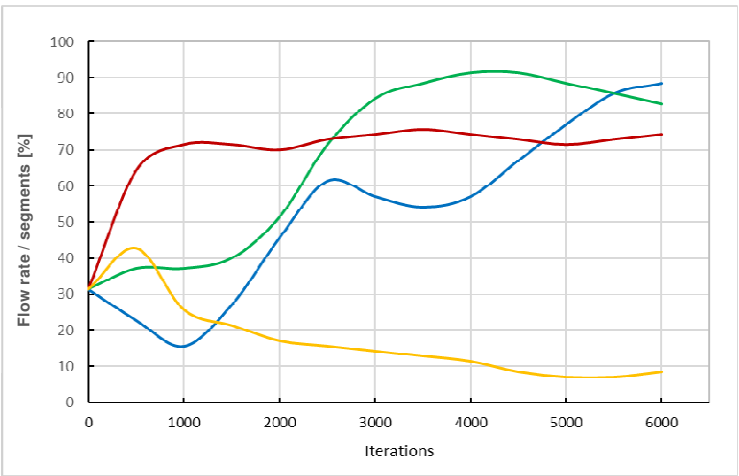


Fig. 2 Graph of convergence of flow rate through significant segments

Fig. 3 displays the temperature profiles at various critical points within the engine. It shows that temperature values generally stabilize quickly, except for the temperature behind the turbine, which initially increases. However, as the computation progresses and the values within the model are refined, even this temperature eventually stabilizes close to the expected value. This pattern demonstrates the dynamic nature of thermal behavior in jet engines and highlights the model's capability to capture significant thermal transitions and stabilize them as part of the convergence process.

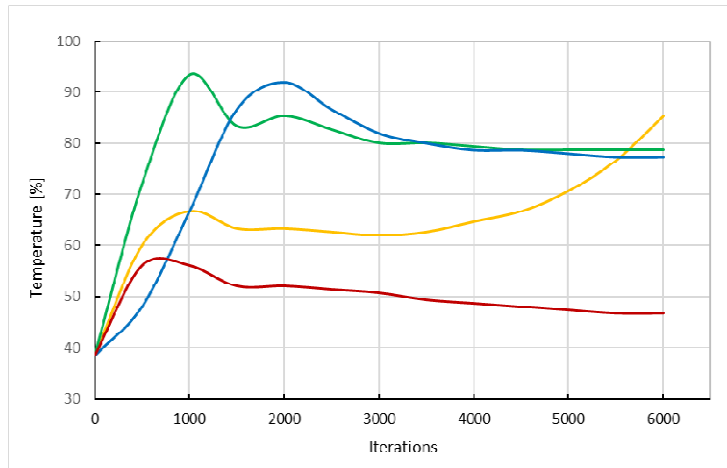


Fig. 3 Graph of convergence of temperature on significant planes

From the graphs, it can be observed that convergence only begins after 6 000 iterations. These early iterations capture the most significant adjustments in the simulation, where major divergences or instabilities would appear. Later iterations primarily serve to confirm the stable convergence of the simulation. Acceptable stability in the computation is achieved after 10 000 iterations, and the calculation can be considered complete after approximately 15 000 iterations.

Fig. 4 displays positions of significant surfaces for graphs on Figs 2 and 3.

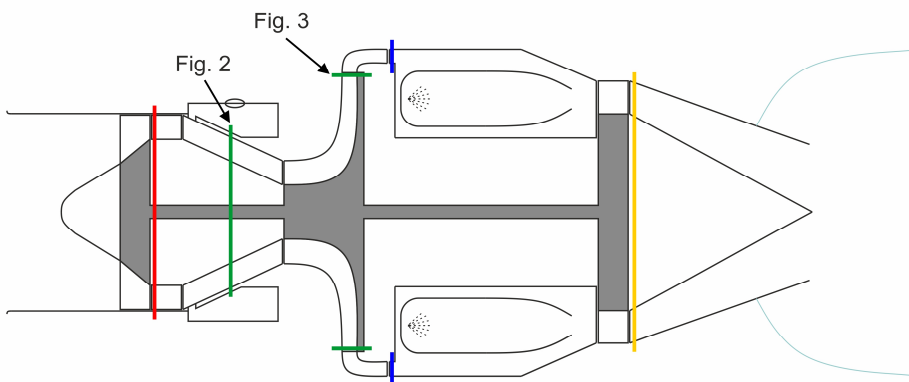


Fig. 4 Positions on significant surfaces for Figs 2 and 3

The initial values shown at the start of the iterations in Figs 2-5 represent the starting points of various physical quantities. These values are set at different percentages due to confidentiality reasons related to the protection of industrial property, and specific numerical details cannot be disclosed. These starting values are essential for understanding the relative changes and trends observed during the simulation iterations.

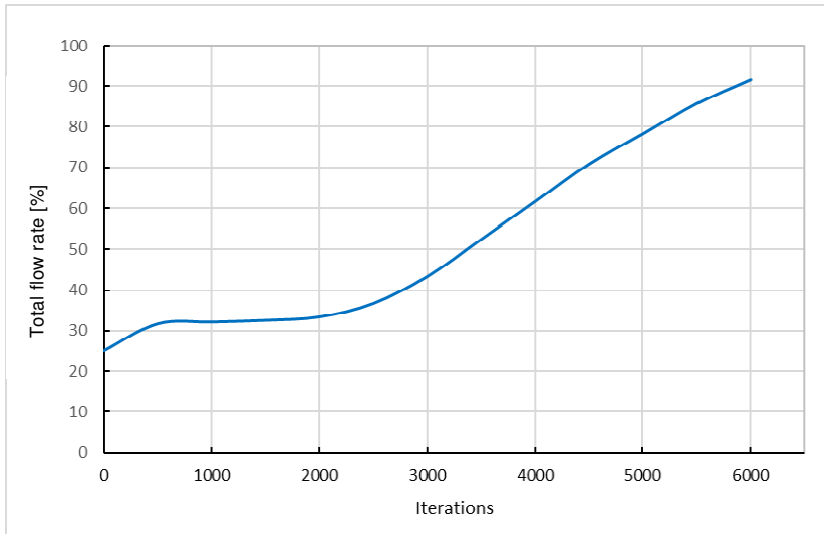


Fig. 5 Graph of convergence of total flow rate through engine

The curves presented in Figs 2-5 are displayed up to 6000 iterations because this initial phase of the computation is the most critical. For experienced computational engineers, this early segment of the simulation is indicative of whether the calculation will converge and whether it is worthwhile to continue awaiting its completion. In many instances, physical quantities, typically pressure or temperature, may spike to implausibly high values. Even if the simulation continues to run under these conditions, such behavior clearly lacks physical validity. The trend of these curves provides insight into whether the computation is converging properly and justifies further computational effort.

The observed trends in the compression ratios of the radial and axial compressors, as depicted in Fig. 6, are a result of the convergence behavior of individual variables. The compression ratios are calculated based on pressures, and it typically takes several thousand iterations for these values to stabilize at their correct levels. The initial divergence in compression ratios between the radial and axial compressors can be attributed to their different operational dynamics and the complex interactions within the engine model as it approaches a converged state.

3 Results and Discussions

The results of the compression calculation on the axial and radial compressors were consistent with the individual segment computations and aligned with the design specifications. Therefore, the calculation of the complete engine can be considered successful.

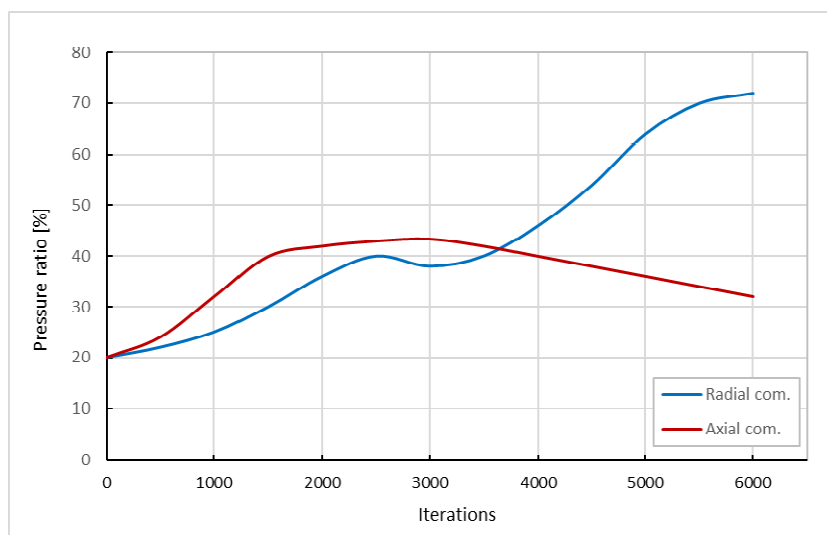


Fig. 6 Graph of convergence of compression rate on each compressor

The expansion ratio value obtained from the turbine in the complete model corresponded to the expansion ratio value calculated for the individual turbine segment. This value also matched the expected value from the design specifications.

The flow characteristics within the combustion chamber in the complete model were compared to those of the standalone combustion chamber model, and they exhibited agreement.

Based on the comparison of all available simulation results and the design specifications, it can be concluded that the model of the complete jet engine was successfully created, and the computation yielded favorable outcomes.

Due to the active development and confidentiality of the jet engine, it is not possible to present specific images, graphs, or figures as they would disclose sensitive information. The author has successfully created a functional numerical model of a complete jet engine, including the simulation of combustion processes, which in itself is no trivial achievement. The article outlines the methodology used to develop this model and illustrates the computational behavior during convergence phases. None of these steps should be considered trivial or taken for granted. The developed model can be further utilized for optimization and studying the behavior of the entire engine, provided that sufficient computational resources are available.

One significant drawback of this model is its size, complexity, and the subsequent computational demands it imposes. However, once the appropriate modeling approach, individual component configurations, and computation settings are established, it becomes feasible to explore the engine's behavior under various flight conditions. Undertaking such computationally intensive work necessitates access to sufficient computational power.

Fig. 7 presents a visualization of the TJ-200 engine, as featured on the official website of PBS Velká Bíteš during the article revision process.



Fig. 7 Visualization of engine TJ-200 from official website www.pbs.cz

4 Conclusions

After approximately nine months of work, the creation and computation of a comprehensive model (including combustion) of the complete jet engine have been successfully achieved.

The development of individual segments and their integration was derived from the author's previous work and proved to be relatively straightforward.

The most challenging aspect involved finding the appropriate configuration for the combustion model to ensure convergence of the computation and accurate representation of the desired variables. This phase consumed the most time and posed the greatest difficulty.

This developed model can be utilized to study the behavior of individual engine components under various flight conditions, optimize specific parts, and improve operational parameters.

Thanks to this model, it becomes possible to efficiently optimize individual engine components and observe how changes in one part affect the performance of the entire engine. This substantial advantage, however, is counterbalanced by the complexity and demands associated with successfully assembling the complete model.

The next step will involve constructing a complete jet engine model without relying on periodicity. By avoiding interfaces like the mixing-plane between segments, where errors can arise, we will have the ability to incorporate non-periodic features into the geometry of the model, such as struts, probes, or control valves. The current model incorporates all essential components necessary for the complete functionality of the engine. Only certain non-periodic components, which do not critically influence the overall function, were omitted. For the initial version of this comprehensive and complex model of a dual-stage jet engine, this simplification was deemed satisfactory and is a common practice in the field. Unfortunately, such a model will entail a mesh element count in the tens of millions, but its accuracy and capability to capture additional physical phenomena will be significantly enhanced.

Acknowledgement

I would like to express my gratitude to my colleagues from PBS Velká Bíteš a.s. for their invaluable expertise and assistance in the development and computation of this

model. Their contributions have been instrumental in the successful creation and analysis of the model, and their support has been indispensable throughout the entire process.

References

- [1] BRIONES, A.M., A.W. CASWELL and B.A. RANKIN. Fully Coupled Turbojet Engine Computational Fluid Dynamics Simulations and Cycle Analyses Along the Equilibrium Running Line. *Journal of Engineering for Gas Turbines and Power*, 2021, **143**(6), 061019. DOI 10.1115/1.4049410.
- [2] LEE, D., H. CHUNG, Y.S. KANG and D.H. RHEE. A Study of an Integrated Analysis Model with Secondary Flow for Assessing the Performance of a Micro Turbojet Engine. *Applied Sciences*, 2024, **14**(7), 7606. DOI 10.3390/app14177606.
- [3] IBING X., Y. CHONG and P. YING. Analysis of Discrepancies Between 3-D Coupled and Uncoupled Schemes Based on CFD In Full Engine Simulation. *Aerospace Science and Technology*, 2022, **131**, 107978. DOI 10.1016/j.ast.2022.107978.
- [4] KONECNY, P. and R. SEVCIK. Comparison of Turbulence Models in Open-FOAM for 3D Simulation of Gas Flow in Solid Propellant Rocket Engine. *Advances in Military Technology*, 2016, 11(2), pp. 239-251. DOI 10.3849/aimt.01131.